



## HIGH TEMPERATURE WEAR BEHAVIOUR OF FE-BASED MATERIALS

E. Badisch<sup>1</sup>, H. Winkelmann<sup>1</sup>, M. Kirchgaßner<sup>2</sup>, N. Gostovic\*<sup>3</sup>

<sup>1</sup> AC<sup>2</sup>T research GmbH, Viktor Kaplan-Straße 2, 2700 Wiener Neustadt, Austria

<sup>2</sup> Castolin Ges.m.b.H., Brunner Straße 69, 1230 Vienna, Austria

<sup>3</sup> Messer Tehnogas AD, Banjicki Put 62, 11090 Belgrade, Serbia

**Abstract:** In many industrial segments such as steel or fire clay industry Fe-based hardfacing alloys are widely used to protect machinery equipment exposed to different loading situations where abrasives play a dominating role. In view of the above, 2 Fe-Cr-C hardfacing alloys additionally alloyed with Nb, Mo and B to ensure improved performances at elevated temperature were deposited onto mild steel under optimised gas metal arc welding (GMAW) condition. High-temperature erosive wear (so called HT-ET, 2-body condition) of the hardfacings was evaluated for four different temperatures, for two different impact angles and at one impact velocity. For 3-body impact/abrasion conditions a special designed high-temperature continuous impact/abrasion Tester (so called HT-CIAT) was used. The wear behaviour of the hardfacing was compared with an austenitic steel typically used in high temperature applications. Results indicate that 2-body erosive wear rate of the hardfacing increases with increase of test temperature and impact angles, whereas wear behaviour of the austenitic stainless steel is non-sensitive to the testing temperature. In 3-body impact abrasion testing similar behaviour can be seen; cyclic tests in HT-CIAT at enhanced temperatures result in breaking of coarse carbides, whereas wear mechanisms of the austenitic steel are found to massive abrasion and formation of mechanically mixed layers (MML).

\*Presenting Author

**Keywords:** 2-body erosion, 3-body impact abrasion, high-temperature wear, Fe-Cr-C hardfacing

### 1. INTRODUCTION

Combined wear at high temperatures comprising erosion, impact and abrasion is heavily influencing maintenance costs in many industries. Crusher systems for sinter cake in steel production plants (Fig. 1) or delivery screws are typical examples for such a tribological environment.



**Figure 1.** Heavy duty equipment exposed to high temperature abrasion and impact: Sinter crusher rotor and crusher bars

The material removal mechanisms in such cases are often superposed by the effect of oxidation [1, 2]. The state-of-the-art of erosive wear at elevated temperature has been reviewed comprehensively [3]. Hardfacing of bulk materials is one of the methods to modify surfaces and the tribological performances without changing the bulk properties of components.

Important hardfacing alloys are Fe-Cr-C and Fe-C-B [4, 5]. In this method of surface modification, both the coating and the substrate material is melted giving rise to a good metallurgical bond between the coating and the substrate.

Rapidly solidified fine crystalline microstructure containing finely distributed hard carbide phases can exhibit an excellent combination of hardness and toughness [6]. To achieve high impact resistance of carbide reinforced materials, good ductility and sufficient interfacial carbide-matrix

bonding is necessary [4]. To achieve high abrasion resistance, coarse hard phases and high hardness are important, especially that the hardness of the hard phases and/or the hardness of the matrix are higher than the hardness of the abrasive [7, 8]. Materials with high temperature resistance and oxidation resistance are reported in [9] to high alloyed matrix especially austenites which behave well.

In view of the above, two different Fe-Cr-C hardfacing alloys have been investigated regarding their behaviour under 2-body and 3-body conditions at elevated temperatures with the aim to understand the wear mechanisms on a basic level. Wear behaviour has been compared to a standard austenitic stainless steel for clarification of the influence of hardness and hard phase content on wear behaviour.

## 2. EXPERIMENTAL DETAILS

### 2.1 Materials and characterization

Within this study, a Fe-Cr-C hypereutectic alloy (coarse microstructure), a Fe-Cr-C-B complex alloy (fine microstructure) and a standard austenitic stainless steel have been investigated. Chemical composition and hardness of these materials are summarized in Tab. 1. Typical microstructures of the materials are presented in Fig. 2. Characterisation of microstructure was performed by optical microscopy (OM) after etching and scanning electron microscopy (SEM + EDS). Hardness measurements were carried out with a standard Vickers hardness technique HV5. To determine the hardness of each phase in the microstructure, e.g. hard particles and metallic matrix, micro-hardness HV0.1 was used.

The different hardfacing alloys produced as flux cored wires on iron basis (Tab. 1) were welded onto mild steel plates (DIN 1.0038) with a dimension of  $150 \times 100 \times 6$  mm. Welding parameters were kept constant for all hardfacing alloys investigated [5], which are optimised related to the welding behaviour in practical welding procedures done. The Fe-Cr-C hypereutectic alloy consists of primary Fe/Cr carbides in a ledeburitic matrix (Figure 2a). The content of Fe/Cr carbides was reported in [5] to be 57.1 % with size of 30-200  $\mu\text{m}$ . The chemistry of the Fe/Cr carbides is reported for hypereutectic Fe-Cr-C alloys in literature to be  $\text{M}_7\text{C}_3$  structure [10]. The hardness is determined to 880 HV5. More details on microstructure are reported in previous investigations by the authors in [5].

Fe-Cr-C-B complex alloy shows a dense and uniform distribution of very hard complex carbides and carbo-borides (Fig. 2b) with hardness values

between 1200 and 1900 HV0.1. The hard phases were identified as Fe/Cr carbo-borides with a volume content of 52% and a size of 10-100  $\mu\text{m}$ , Nb carbides and Mo/W carbo-borides with a volume content of approximately 5% in blocky shape [5]. In addition, the hardness of the matrix is also very high which is reflected by a hardness of 1020 HV5. This is due to a nanocrystalline microstructure of the matrix, both improving toughness and hardness [5].

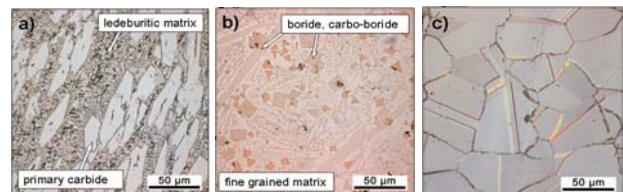


**Figure 2.** Microstructure of the materials investigated. **a)** Fe-Cr-C hypereutectic, **b)** Fe-Cr-C-B complex Nanoalloy®, **c)** austenitic

The austenitic steel (Fig. 2c) which has a heat resistant microstructure at C-content of 0.08 %, Cr-content of 25 % and 20 % Ni. Hardness of this material was determined to 175 HV5. Austenitic stainless steels have high ductility, low yield stress and relatively high ultimate tensile strength, when compared to typical carbon steel. Austenitic steels showing fcc-structure, which provides more planes for the flow of dislocations, when combined with the low level of interstitial elements, give this material a good ductility.

**Table 1.** Chemical composition of the materials investigated.

Material	Chemical composition [wt.-%]						Fe
	C	Cr	Ni	Nb	B	Others (Mo, V, W)	
Fe-Cr-C hypereutectic alloy	5.5	21.0	-	7.0	-	10.0	base
Fe-Cr-C-B complex alloy	1.3	15.4	-	4.2	4.2	11.5	base
Austenitic stainless steel	0.08	24.8	19.8	-	-	-	base

### 2.2 High-temperature erosion test (HT-ET) - 2-body erosion

Solid particle erosion tests have been performed in a conventional centrifugal four-channel accelerator where up to 20 specimens can be treated simultaneously under identical testing conditions (Fig. 3a). Testing parameters used are given in Tab. 2. The abrasive particles used in this work were angular silica particles at a grain size of 0.1 - 0.3 mm. Investigation of steady state erosion rate was made as a function of the impact angle at the abrasive particle velocity of 80 m/s. Erosion tests were conducted at impact angles of 30° and 90°, respectively. To study erosion at elevated temperature, the centrifugal apparatus was put into the heated test chamber where tests at enhanced

temperatures were carried out at 300, 500 and 650°C. The erosion rate was determined as a volume loss of the target sample per mass of abrasive particles impinging the target (mm<sup>3</sup>/kg). An accuracy of 0.1 mg was obtained for the target mass loss measurements. Each wear test was repeated for three times.

**Table 2.** Testing parameters used in HT-ET

Parameter	Value
Impact velocity	80 m/s
Impact angles	30, 90°
Erodent	Silica sand, 0.1 - 0.3 mm
Total weight of erodent	6 kg
Test temperatures	RT, 300, 500, 650°C

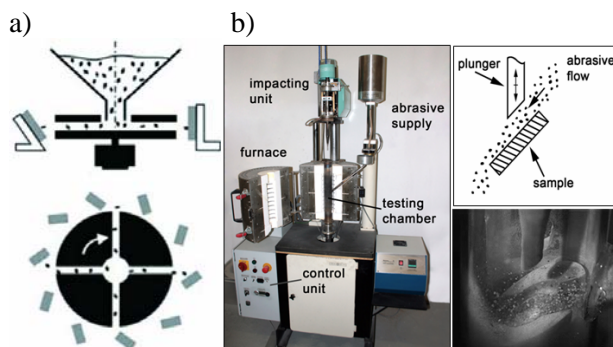


**Figure 3.** View of the wear testing apparatus used within this study. **a)** High temperature erosion test (HT-ET), **b)** High temperature continuous impact abrasion test (HT-CIAT).

The morphologies of the eroded samples are examined with the help of scanning electron microscopy (SEM) to understand the material removal mechanism. The eroded samples are then sectioned along a plane perpendicular to the eroded surface. The sectioned surfaces were then polished and observed under optical microscopy to assess the nature of subsurface deformation and various coatings formation.

### 2.3 High-temperature continuous impact abrasion test (HT-CIAT) - 3-body impact abrasion

The HT-CIAT was developed by Castolin and AC<sup>2</sup>T to determine the behaviour of materials in continuous impact abrasive environment at elevated temperatures. Test principle is simply based on potential energy which is cyclic turned into kinetic energy by free fall. The samples are fixed in 45° and get continuously hit by the plunger, while a constant abrasive flow is running between the sample and the plunger as shown in (Fig. 3b). Impact energy, angle of impact and frequency were chosen as 0.8 J, 45° and 2 Hz, respectively. The total number of testing cycles was fixed to 7.200 which correlate to a testing duration of 1 hour. The abrasive material used for 3-body-contact was silica

sand with a particle size of 0.4-0.9 mm at angular shape and a flow rate of 3 g/sec. Experiments were carried out at room temperature and 600°C, respectively. The plunger material used at these tests was a Co-rich high speed steel. Characterisation of wear behaviour was done by measuring the weight loss of the samples (accuracy, 0.1 mg), by standard optical microscopy (OM) and scanning electron microscopy (SEM). Also cross-sections images of the worn specimen area have been made to analyse the predominant mechanisms e.g. carbide breaking, cold work hardening, composite layer formation and changes in the matrix caused by high temperature.

## 3. RESULTS AND DISCUSSION

### 3.1 HT-ET results and discussion

The dependence of the volumetric erosion rate of all materials investigated on the test temperature is shown in Fig. 4 for glancing impact angle. In general, it can be observed that the erosion rate of all three materials increases at higher testing temperature. This behaviour can be explained by softening effects which get dominant at higher temperatures.

The increase in erosion resistance of the austenitic could be due to the precipitation of additional Cr-carbides at temperatures above 500°C which is usual for not stabilised austenitic steels [19]. A good correlation of erosion rate and material hardness can be detected at room temperature where the softest austenite (175 HV) shows highest erosion rate compared to the hardest Fe-Cr-C-B complex (1020 HV) which behaves best.

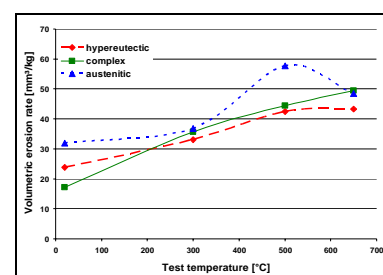


**Figure 4.** Volumetric erosion rate in dependence of test temperature for all materials investigated in HT-ET (impact angle, 30°).

The variation of erosion rate of all three materials as function of temperature under normal impact condition is presented in Fig. 5. It can be seen that the erosion rate of all three materials is at room temperature in the same range, whereas at enhanced temperature complete different behaviour can be observed. For Fe-Cr-C hypereutectic and Fe-Cr-C-B complex the erosion rate increases with the test temperature. However, in case of the austenite,



the erosion rate remains more or less independent on the test temperature on a low level. Therefore, significant differences in erosion rate by a factor 4-5 are shown at highest test temperature of 650°C (Fig.5).

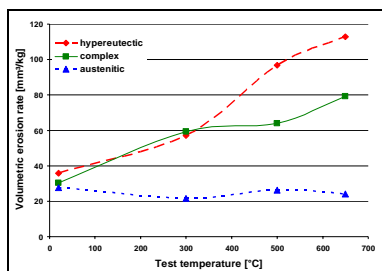


**Figure 5.** Volumetric erosion rate in dependence of test temperature for all materials investigated in HT-ET (impact angle, 90°).

In Fig.6 the typical worn austenitic surface at 30° impact angle tested at room temperature indicates a highly plastically deformed surface where pronounced abrasion grooves can be observed. This ductile behaviour which is well known for austenitic materials in combination with the relatively low material hardness is responsible for highest wear rate of all materials tested at room temperature under glancing impact angle.

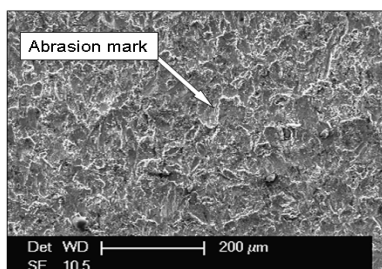


**Figure 6.** SEM micrograph of a typical worn austenitic surface after erosion testing at room temperature (impact angle, 30°).

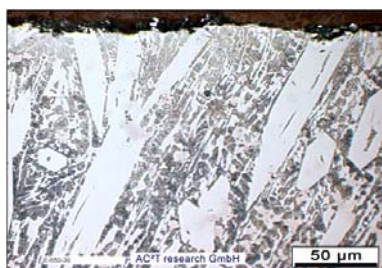


**Figure 7.** Cross-section image of a typical worn surface of Fe-Cr-C hypereutectic after erosion testing at 650°C (impact angle, 30°).

The wear behaviour of the Fe-Cr-C complex under highest test temperature of 650°C can be observed in the cross-section image in Fig. 7. There, the eroded surface which is worn very uniform in the coarse multiphase microstructure can be seen. Coarse primary carbides as well as ledeburitic matrix get worn in a simultaneously behaviour, whereas no significant cracking in

carbides or interface matrix/carbide can be seen. Because of this, the erosion rate at 650°C is only on slight enhanced level compared with room temperature tests (Fig. 4).

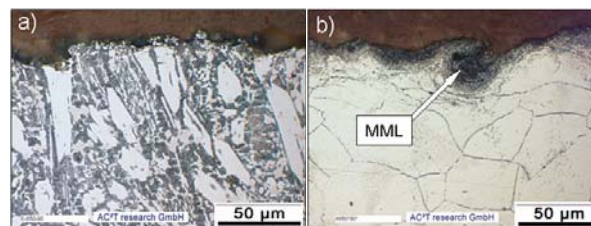


**Figure 8.** Typical cross-section images after erosion testing at 650°C and 90° impact angle. a) Fe-Cr-C hypereutectic, b) austenitic.

Erosion mechanisms for normal impact at 650°C are presented in the cross-section images in Fig. 8. The very high erosion rate of the Fe-Cr-C hypereutectic described in Fig. 5 can be explained clearly with Fig.8a. There, the predominant material removal mechanism is given to brittle fracture of coarse primary carbides in the ledeburitic matrix. This behaviour can be explained by insufficient mechanical support of the carbides by the ledeburitic matrix due to softening effects at these high temperatures [11]. Compared to the high erosion level of Fe-Cr-C hypereutectic at 650°C, the austenite shows a temperature independent behaviour on a low erosion level. A typical cross-section image after testing is given in Fig. 8b. There, a highly plastically deformed near surface zone of approximately 50 µm in combination with SiO<sub>2</sub> particles form a so called mechanically mixed layer (MML). This in-situ formation of the MML strengthens the austenitic surface and protects the materials against wear.

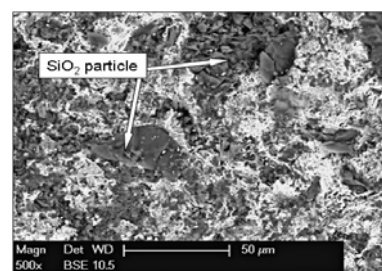


**Figure 9.** SEM of a typical worn austenitic surface after erosion testing at 650°C (impact angle, 90°).

In the eroded surface of Fig. 9, embedded abrasives particles can be seen clearly. The content of SiO<sub>2</sub> within the eroded surface can be seen on the dark zones in the back-scattering SEM image (BSE) which correspond to non-metallic particles. A high content of approximately 50 % of the eroded surface is covered with abrasive particles sticking on the surface and forming a mechanically mixed layer. This is in good correlation with previ-

ous investigations reported in [11]. It was observed that the formation of the MML is more pronounced at higher temperatures which can be explained by the higher ductility of the austenitic material at enhanced temperatures and therefore preferred which prefers embedding of abrasive particles.

### 3.2 HT-CIAT results and discussion

Volumetric wear of the materials investigated in 3-body impact abrasion at room temperature and 600°C is given in Fig.10. Results at room temperature testing show very low wear of approximately 3 mm<sup>3</sup> for coarse multiphase materials containing large amount of hard phases. Increased wear can be detected for the austenite which can be explained by lowest hardness and lack of hard phases in the microstructure. HT-CIAT at 600°C indicates increased wear for all of the materials investigated, whereas Fe-Cr-C hypereutectic with the coarse carbides shows an increase of wear by a factor of four compared to room temperature testing (Fig. 10). Better performance can be observed for the fine-grained microstructure of Fe-Cr-C-B complex which is explained in [4] to have better matrix-carbide interfacial bonding. Increased wear can be also detected for the ductile austenite at 600°C because of insufficient coarse hard phases which can withstand against abrasive environments especially at enhanced temperatures when the matrix gets softening.

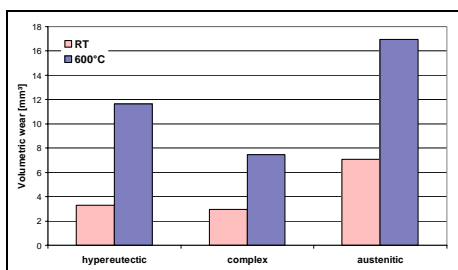


**Figure 10.** Volumetric wear of all materials investigated in HT-CIAT (testing temperature, room temperature and 600°C)

Typical macro images of worn surfaces after HT-CIAT are listed in Fig. 11 where the influences of testing temperature and microstructure are present. It can be seen that for Fe-Cr-C hypereutectic, representative for high hard phase content, tested at room temperature (Fig. 11a) only low grooving of the surface takes place which is in good agreement with the low wear in Fig. 10. At higher temperatures the grooving mechanisms is more pronounced resulting in higher wear (Fig. 11b). Different behaviour can be detected for the austenite containing no hard phases. This material has two different wear mechanisms which are seen in the macro image in Fig. 11c. In the impacting

zone, the formation of a mechanically mixed layer takes place (upper part in Fig. 11c), and in the abrasion dominating region (lower part in Fig. 11c) massive abrasion with deep grooving is present.

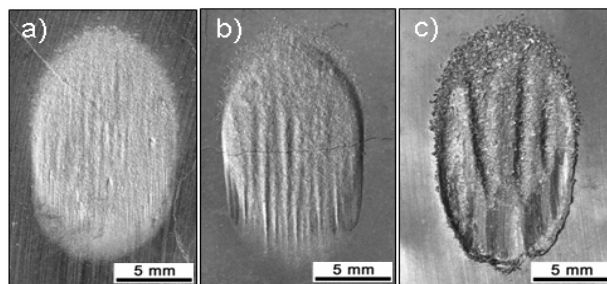


**Figure 11.** Macro images of typical wear tracks after HT-CIAT. **a)** Fe-Cr-C hypereutectic (room temperature testing), **b)** Fe-Cr-C hypereutectic (testing temperature, 600°C), **c)** austenitic (testing temperature, 600°C)

For deeper understanding of the mechanisms interacting with the microstructure detailed SEM investigations were done. Fe-Cr-C-B complex representative for materials with high hard phase content the worn surface tested at room temperature is given in Fig. 12a. It can be seen that no significant fracture and breakouts are present. Only low tendency to plastic deformation and SiO<sub>2</sub> particle sticking can be detected. At enhanced testing temperature the wear behaviour is changing where abrasion marks and highly deformed areas can be detected (Fig. 12b). Protruding carbides also break at higher temperatures due to fatigue and by the worse matrix backing which is due to softening at higher temperatures.

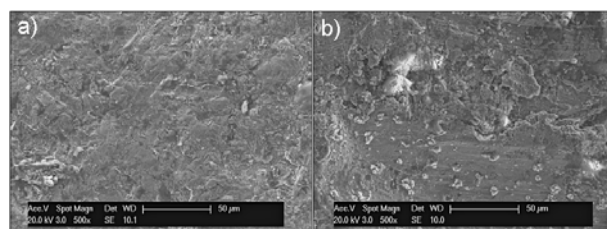


**Figure 12.** SEM micrographs of typical worn surfaces of Fe-Cr-C-B complex after CIAT. **a)** testing at room temperature, **b)** testing temperature, 600°C

The wear behaviour of the austenite is governed by the formation of a MML in the impacting dominating zone. SiO<sub>2</sub> particles are embedded into the highly plastically deformed austenitic surface (Fig. 13a) resulting in an in-situ increase in wear resistance. It was observed that the tendency of MML formation which is also thicker is more pronounced at higher temperature because of the higher plasticity at these temperatures. In the abrasion dominating region (lower area in Fig. 11c) the wear behaviour is controlled by massive abrasive grooving and chipping which result in increase wear rates in HT-CIAT. At high temper-

atures, when the matrix gets softening, a certain amount of coarse hard phases are necessary to withstand grooving and therefore keep the wear on a low level.

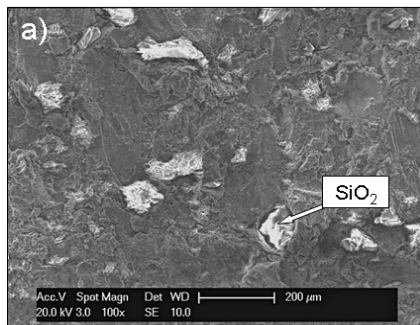


**Figure 13.** SEM micrographs of typical worn austenitic surfaces after CIAT at 600°C.

a) impacting zone, b) abrasive dominated region.

#### 4. CONCLUSIONS

Based on the investigations within this work, following conclusions can be drawn:

1. Coarse microstructure with carbides performs well under glancing impact angle, whereas brittle behaviour is observed at normal impact angle in erosion test.

2. Single phase austenitic materials show ductile behaviour and in-situ formation of mechanically mixed layers (MML) which is more pronounced at higher temperatures which enables a temperature independent behaviour under normal impact angle.

3. Breaking of coarse hard phases at high temperatures takes place due fatigue effects and insufficient mechanical support by the matrix.

4. In abrasion conditions, a certain content of hard phases is necessary to keep wear on a low level, therefore a pure austenitic structure is not favourable in case such conditions appear at least in certain areas of the loaded parts.

5. In impacting loading conditions, a coarse microstructure is a disadvantage.

6. As future development direction austenitic structures reinforced with hard phases could be of high interest.

7. Complex Nanoalloys® are state of the art for protection under combined wear with a dominant abrasive component where austenitic materials have much less wear resistance.

#### ACKNOWLEDGEMENTS

This work was funded from the "Austrian Kplus-Program" (governmental funding program for pre-competitive research) via the Austrian Research Promotion Agency (FFG) and the TecNet Capital GmbH (Province of Niederösterreich) and has been carried out within the "Austrian Center of Competence for Tribology" (AC<sup>2</sup>T research GmbH). The authors are also grateful to Böhler Edelstahl for supporting starting materials and performing heat treatment procedures at different steel types and to Castolin Eutectic for helpful work in manufacturing of welding samples.

#### REFERENCES

- [1] Roy M, Ray KK, Sundararajan G. Erosion-oxidation interaction in Ni and Ni-20Cr alloy. *Metal and Mater Trans* 2001;32A:1431-51.
- [2] Katsich C. Werkstoffverhalten bei erhöhten Temperaturen unter abrasiver Beanspruchung. Master Thesis. University of Leoben 2009.
- [3] Roy M. Elevated temperature erosive wear of metallic materials. *J of Physics D. Appl Physics* 2006;39:101-24.
- [4] Badisch E, Kirchgaßner M, Polak R, Franek F. The comparison of wear properties of different Fe-based hardfacing alloys in four kinds of testing methods. *Tribotest* 2008;14:225-33.
- [5] Kirchgaßner M, Badisch E, Franek F. Behaviour of iron-based hardfacing alloys under abrasion and impact. *Wear* 2008;265:772-9.
- [6] Branagan DJ, Tang Y. Development extreme hardness (>15 GPa) in iron based nanocomposites, *J Compos Part A* 2002;33:855-9.
- [7] Badisch E, Mitterer C. Abrasive wear of high speed steels: influence of abrasive particles and primary carbides on wear resistance. *Tribol Int* 2003;36:765-70.
- [8] Francucci G, Sikora J, Dommarco R. Abrasion resistance of ductile iron austempered by the two step process. *Mater Sci Eng A* 2008;485:46-54.
- [9] Celik O, Ahlatci H, Kayali ES, Cimenoglu H. High temperature abrasive wear behavior of an as-cast ductile iron. *Wear* 2005;258:189-93.
- [10] Chatterjee S, Pal TK. Wear behaviour of hardfacing deposits on cast iron. *Wear* 2003;255:417-25.
- [11] Winkelmann H, Varga M, Badisch E, Danninger H. Wear Mechanisms at High Temperatures: Part 2: Temperature Effect on Wear Mechanisms in the Erosion Test. *Trib Letters* 2009; in press.